TISSUE ENGINEERING: Part B
Volume 21, Number 6, 2015

DOI: 10.1089/ten.teb.2015.0142

Tissue Engineering
& Regenerative Medicine
International Society

REVIEW ARTICLE

Multiscale Biofabrication of Articular Cartilage: Bioinspired and Biomimetic Approaches

Philip David Tatman, BS,[1] William Gerull, BS,[1] Sean Sweeney-Easter, BS,[1] Jeffrey Isaac Davis, BS,[1]
Albert O. Gee, MD,[2] and Deok-Ho Kim, PhD[1,3]

Articular cartilage is the load-bearing tissue found inside all articulating joints of the body. It vastly reduces friction and allows for smooth gliding between contacting surfaces. The structure of articular cartilage matrix and cellular composition is zonal and is important for its mechanical properties. When cartilage becomes injured through trauma or disease, it has poor intrinsic healing capabilities. The spectrum of cartilage injury ranges from isolated areas of the joint to diffuse breakdown and the clinical appearance of osteoarthritis. Current clinical treatment options remain limited in their ability to restore cartilage to its normal functional state. This review focuses on the evolution of biomaterial scaffolds that have been used for functional cartilage tissue engineering. In particular, we highlight recent developments in multiscale biofabrication approaches attempting to recapitulate the complex 3D matrix of native articular cartilage tissue. Additionally, we focus on the application of these methods to engineering each zone of cartilage and engineering full-thickness osteochondral tissues for improved clinical implantation. These methods have shown the potential to control individual cell-to-scaffold interactions and drive progenitor cell differentiation into a chondrocyte lineage. The use of these bioinspired nanoengineered scaffolds hold promise for recreation of structure and function on the whole tissue level and may represent exciting new developments for future clinical applications for cartilage injury and restoration.

Introduction

Articular cartilage is a stratified tissue, comprised of several distinct microscale cellular niches, which vary in both extracellular architecture[1–5] and cell phenotype[6] (Fig. 1). Lacking innervation and direct vascular support, articular cartilage survives through mechanical loading.[2,7–13] Cyclical compression of the articular cartilage matrix facilitates diffusion of nutrients and waste, thus providing the means for chondrocyte homeostasis.[14] Due to its unique extracellular matrix (ECM) composition and collagen architecture, articular cartilage provides a nearly frictionless joint and a stiff load-bearing tissue to absorb the substantial compressive forces that are transmitted through the joint during activity. When the articular cartilage matrix becomes injured, it has a very poor capacity to heal itself. This leads to the formation of inferior fibrocartilage tissue, which has poorer mechanical properties. Often, isolated damage can progress to involve the remaining cartilage and lead to arthritis of the joint.[15–17]

Arthritis is one of the most prevalent musculoskeletal diseases worldwide and is the leading cause of disability in the United States for people over the age of 50.[16,18–20] In 2008, ~30 million people suffered from some form of arthritis and the prevalence is expected to increase to 60 million people by the year 2020.[16] In addition to the pain from articular cartilage loss, many patients experience extensive subchondral bone remodeling.[21–23] Early stage arthritis coincides with an increase of bone density beneath the degrading articular cartilage.[23–26] However, later stage arthritis is characterized by bone erosion due to a complete loss of the overlying articular cartilage.[21,27–29] Multiple clinical treatments to address cartilage injury have been tried, but continue to have significant limitations. They fall short of reconstituting the normal function of the native tissue. Thus, tissue engineering strategies, which combine cells, scaffolds, and biologic stimulation, have been a focus for research in regenerating articular cartilage.

Historically, engineering strategies for replicating cartilage tissue have predominantly revolved around the use of hydrogels. Recent trends have been focused on stratified layers specific to each zone of native cartilage tissue instead of a homogenous biomaterial scaffold.[30,31] By applying a multiscale biofabrication approach, newer scaffolds have been developed that can recapitulate the complex heterogeneous and zonal architecture of native cartilage.

Departments of [1]Bioengineering and [2]Orthopedics and Sports Medicine, University of Washington, Seattle, Washington.
[3]Institute for Stem Cell and Regenerative Medicine, University of Washington, Seattle, Washington.

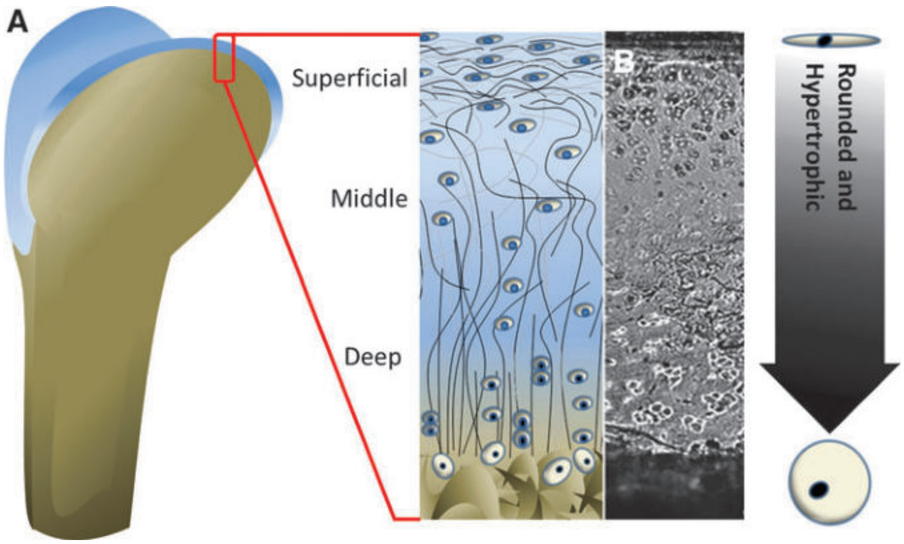

FIG. 1. Ultrastructural organization of native cartilage. **(A)** Illustration representing articular cartilage tissue organization into zones by depth from the surface. Collagen is represented by the *black lines*, while chondrocytes are presented with a *white* soma and *black* nucleus (for visual contrast). Collagen II fibers protrude perpendicularly from the deep bone surface, and progress into a parallel alignment toward the superficial surface. **(B)** Raman mapping reveals the depth-dependent change in chondrocyte morphology and propensity for cells to cluster into dimers.[181] At the superficial surface, chondrocytes have less overall volume and take on a flattened morphology. Chondrocytes exhibit a transition into a hypertrophic morphology with increasing proximity to the surface of bone.

An additional challenge in cartilage tissue engineering is in regenerating the functional interface between bone and cartilage, which is of considerable importance, as this is how new tissue would need to be anchored to the host bone. Many studies have successfully replicated a single element of cartilage; however, no study has successfully mimicked native cartilage with respect to the combination of cartilage matrix organization, physiological and mechanical properties, cell density, and ability to integrate with subchondral bone.

Through a multiscale bioengineering approach, the combination of many techniques have the potential to produce complex 3D tissues mimicking native cartilage and hold great promise in developing new cartilage when implanted *in vivo*. This review aims to summarize recent advances in cartilage tissue engineering and highlight the potential gain of integrating these techniques into a cohesive method to produce a cartilage construct that has clinical translation potential.

Ultrastructural and biochemical characteristics of native articular cartilage

To engineer articular cartilage, it is important to understand the composition, structure, and mechanical properties of the native tissue. The biochemical composition of articular

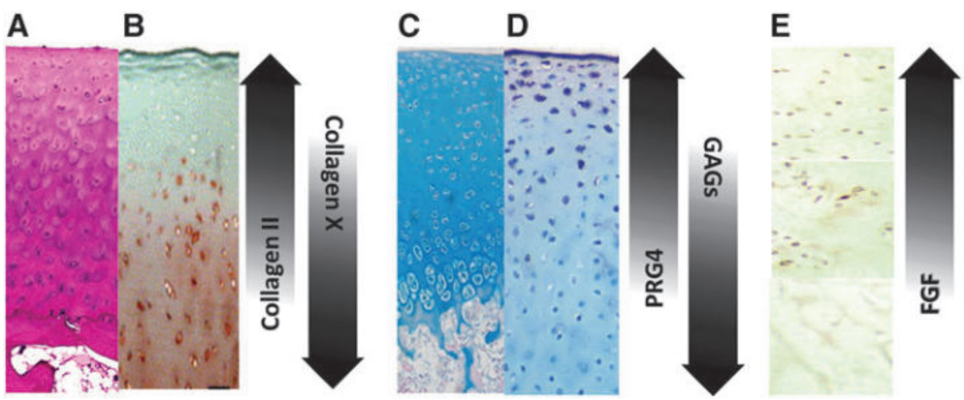

FIG. 2. Biochemical spatial distribution of adult articular cartilage. **(A)** Hematoxylin and eosin staining demonstrates chondrocyte distribution throughout the depth of the tissue.[182] **(B)** Safranin-O staining reveals the distribution of collagen from deep to superficial.[183] **(C)** Alcian blue staining reveals the distribution of GAG and PG in a depth-dependent manner.[182] **(D)** Proteoglycan 4 (PG4) provides a strong marker for physiologic and functional cartilage, as it is expressed in the superficial zone of cartilage in response to mechanical loading.[184] **(E)** The fibroblast growth factor (FGF) family of proteins has been known to progress chondrogenesis and FGF-2 is known to be expressed in resting populations of chondrocytes.[185]

cartilage includes collagen types II and X,[32–34] proteoglycan 4 (PG4) and aggrecan,[35–42] and glycosaminoglycans (GAGs), including chondroitin sulfate, hyaluronic acid (HA), and keratin sulfate.[31,43–47] Four unique zones form the articular cartilage: the superficial, middle, deep, and transition zones.[1,30,31,48] Each of these zones has a unique composition, cell phenotype, and physiological property (Figs. 1 and 2).

The superficial zone has the greatest resistance to shear stress, which allows the contacting surfaces of the joint to slide across one another in a low friction environment,[34,49–51] and supports the joint surface by way of anisotropic arrangement of collagen.[34,52] The collagen is highly ordered into parallel fibers in the direction of applied shear force. This zone has the highest concentration of collagen type II and trace amounts of other collagen types I and III.[33,53] GAGs and proteoglycans do not reside in this layer, with the exception of PG4, which is found in high concentrations (Fig. 2). PG4 functions as a lubricating component in synovial joints.[35,36,54,55] Chondrocytes have the highest density in the superficial zone and take on a flattened morphology[31,48,56,57] (Fig. 1).

Deep to the superficial zone resides the middle zone. The defining feature of the middle zone is the lack of matrix organization. Collagen randomly orients (Fig. 1A), aggrecan and GAGs are present in relatively moderate concentrations, and PG4 concentration is reduced (Fig. 2D).[2,34,40] Physiologically, this zone serves as a transition between the superficial and deep zones and possesses a random orientation of the collagen matrix, which acts as a spongy compressive layer to the impact of mechanical loads.[52] Chondrocytes take on a slightly rounded morphology and are present in a lower density relative to the superficial zone[57–59] (Fig. 1B).

Transitioning to the deep zone, type II collagen fibers orient perpendicular to the superficial layer (Fig. 1A). In addition to type II collagen, type X collagen accumulates to an appreciable degree (Fig. 2A, B).[33] This zone is rich in GAGs and contains a high concentration of aggrecan, while PG4 concentration is negligible[1,2,52,57,58] (Fig. 2C, D). Chondrocytes organize into distinct columns, and often form cell dimers[57] (Fig. 1). The deep zone has the highest resistance to mechanical compression, with a modulus ranging in the order of 10–20 MPa.[52,60] The deepest layer, known as the transition zone or tidemark, has a similar composition as the deep layer with the addition of calcified collagen.[61–63] As the collagen becomes more heavily calcified, the matrix transitions to bone, and the cell phenotype progresses from chondrocyte to osteocyte. This layer anchors the articular cartilage to the underlying subchondral bone.

The composition of articular cartilage and the spatial organization of these components play a major role in cartilage homeostasis.[64–66] In general, PG and GAG content increases with depth while collagen concentration is inversely proportional (Fig. 2A, D). Due to the hydrophilic nature of PG and GAG, and their paucity at the surface of cartilage, an osmotic gradient develops, which favors the movement of water into the cartilage matrix.[2,14,32] Compression of the cartilage matrix, during physiological loading, forces water and waste out, while the osmotic gradient pulls water and nutrients back into the matrix under conditions of low mechanical stress.

The composition of articular cartilage results in unique mechanical properties (Table 1). In the lower extremities of adult humans, articular cartilage has been reported to have an instantaneous compressive modulus ranging from 1 to 19.5 MPa and an equilibrium compression modulus averaging around 1 MPa, depending on the specific joint and surface within each joint[67,68] (Table 1). The Young's Modulus varies from 2 to 4 MPa, and these numbers vary based on the zone and location within each joint[69,70] (Table 1). Chen *et al.* showed that the equilibrium compressive modulus of cartilage increases with depth, from 0.7 MPa in the superficial zone to over 7 MPa in the deep zone.[71] Additionally, Barker and Seedhom utilized different cartilage plugs from different areas in the human knee to show that the instantaneous compressive modulus increases medially and laterally from the center of the joint.[72] Shepherd and Seedhom further demonstrated the variance of human cartilage properties by characterizing the instantaneous compressive modulus in each joint of the human lower limbs, the talar cartilage having the highest (10.6–18.6 MPa), while the knee and hip were essentially equal (5.5–11.8 MPa).[68]

History and Present State of Hydrogel Engineering Applied to Articular Cartilage

Previous work toward engineering articular cartilage has predominantly focused on the use of various hydrogel scaffolds. Hydrogels have several advantages, including ease of formation, a consistent cellular distribution, ability to tune mechanical properties, and ability to control polymer composition. These properties allow hydrogels to be customized to specific engineering criteria. In the context of articular cartilage engineering, hydrogel engineering has evolved over time to be able to recapitulate many components of cartilage tissue. These studies have demonstrated important interactions between the engineered components of a hydrogel and its encapsulated cells at the nanoscale level.

Early studies, which applied the use of hydrogels to cartilage engineering, found that the micro and nanoarchitecture of a hydrogel could be engineered to manipulate cell migration,[73,74] gene transcription,[75–77] ECM formation,[78–80] and stem cell differentiation.[81–84] Bryant *et al.* showed that crosslinking density of PEG hydrogels is directly correlated to hydrogel pore size,[80] and subsequent studies have shown that chondrocytes deposit more ECM in gels with relatively larger pore size.[76,78,79,85] Although, it has also been observed that gels with higher density and smaller pore size upregulate metalloproteases, which are chondrogenic markers associated with increased matrix catabolism.[76] With respect to stem cell differentiation, small nanoscale wrinkles on the surface of a PEG hydrogel have been shown to differentiate mesenchymal stem cells (MSCs) into osteocytes,[82] polymer macromere density has supported MSC differentiation into chondrocytes,[83] and recently controlling the mean size of pores in a hydrogel has also been shown to determine the degree to which MSC differentiate into chondrocytes.[84] These studies highlight the nano and microscale interaction hydrogels have with encapsulated cells and thus the need to consider multiple layers of scale when engineering hydrogels for cartilage engineering.

TABLE 1. MECHANICAL PROPERTIES OF ARTICULAR CARTILAGE DETERMINED IN VARIOUS JOINTS THROUGHOUT THE HUMAN BODY

Mechanical properties of human cartilage				
Author	*Test*	*Area*	*Value (Mpa)*	*Conclusion*
Shepherd *et al.*[68]	Instantaneous compression modulus	Ankle (mean of all cart.)	13.49	Mean compression: 9.90 Mpa
		Knee (mean of all cart.)	8.29	
		Hip (mean of all cart.)	7.98	Mechanical properties change with location in the body
Barker and Seedhom[72]	Instantaneous compression modulus	Medial femoral condyle (mean)	12.36	Mean compression, all data: 10.00 Mpa
		Lateral femoral condye (mean)	17.47	
		Medial tibial condyle (mean)	14.80	Mechanical properties vary within a given articular joint and location in the body
		Lateral tibial condyle (mean)	10.73	
		Medial patellar surface (mean)	7.27	
		Lateral patellar surface (mean)	8.63	
		Medial tibial plateau: in contact w/femur (mean)	3.57	
		Lateral tibial plateau: in contact w/femur (mean)	4.60	
Roberts *et al.*[193]	Instantaneous compression modulus	Anteroinferior femoral head	9.7 (3.6)	Mean compression: 11.4 Mpa
		Zenith, femoral head	13.1 (3.6)	Mechanical properties vary within a given articular joint
Chen *et al.*[71]	Equilibrium compression modulus	Femoral head	2.72 (0.86)	Compressive modulus varies across tests.
	Equilibrium bulk compression modulus	Femoral head	1.18 (0.26)	Mechanical properties vary within the depth of articular cartilage
Treppo *et al.*[67]	Equilibrium compression modulus	Talar cartilage	0.8 (0.05)	Mean compression: 0.6 Mpa
		Tibial plateau	0.4 (0.25)	Mechanical properties vary with changes to cartilage water content
Huang *et al.*[70]	Equilibrium compression modulus	Humeral head	0.141 (0.48)	Mean compression (equilibrium modulus): 0.160 Mpa
		Glenoid	0.178 (0.094)	
	Tensile Young's modulus	Humeral head	4.23 (2.88)	
		Glenoid	2.24 (2.93)	Mean compression (Young's modulus): 3.24 Mpa; Mechanical properties vary within a given articular joint
Kurkijärvi *et al.*[69]	Tensile Young's modulus	Femoral groove	1.00 (0.43)	Mean compression: 0.90 (0.43) Mpa
		Femoral medial condyle	1.16 (0.36)	
		Tibial medial plateau	0.84 (0.41)	Mechanical properties change with location in the body
		Anterolateral patellae	0.56 (0.24)	
		Femoral lateral condyle	1.10 (0.48)	
		Tibial lateral plateau	0.78 (0.38)	
Sweigart *et al.*[194]	Equilibrium compression modulus	Anterior femoral	0.15 (0.03)	Mean compression: 0.12 Mpa
		Central femoral	0.10 (0.03)	
		Posterior femoral	0.11 (0.02)	Mechanical properties vary within a given articular joint
		Anterior tibial	0.16 (0.05)	
		Central tibial	0.11 (0.04)	
		Posterior tibial	0.09 (0.03)	

Further advances in hydrogels have demonstrated an ability to control protein diffusion and sustained release of growth factors, which influences encapsulated cells. This phenomenon is a result of the properties of the hydrogel. A study using encapsulated beta-islet cells in different densities of PEG found that in response to a glucose stimulus, the encapsulated cells exhibited the same accumulative response of insulin secretion, but the insulin was released from the hydrogel at different rates depending on the degree of crosslinking, thus demonstrating a relationship between hydrogel crosslinking and control of protein diffusion.[86] Additional studies by Engberg and Frank revealed that the size of protein permitted to diffuse through a hydrogel can also be controlled, and by using PEG, demonstrated control over globular proteins up to 10.7 nm in diameter.[87] These studies show that the properties of hydrogels control the diffusion of proteins on the order of nanometers. The ability to control protein diffusion within a hydrogel occurs using many different types of polymer including: chitosan,[88] thermosensitive organophosphazene,[89] self-assembling peptides (SAPs),[90] and gelatin.[91] Many of these principles have been applied to cartilage tissue engineering to enhance tissue formation.[92–94]

Another important element of hydrogels is the choice of polymer. In addition to PEG and other synthetic polymers, many natural biopolymers can be readily synthesized and used to form hydrogels. Gelatin,[95–99] collagen,[89,100–102] chondroitin sulfate,[103–105] HA,[81,106,107] and chitosan[88,108–111] are just a few examples of biological polymers that have been adapted into hydrogels. Using biopolymers has several advantages over synthetic polymers, the most obvious being achieving a closer resemblance to native tissue. These biopolymers can stimulate stem cell differentiation[81,83,101] and intercellular signaling through the binding of cell surface receptors. In this manner, biopolymers have been shown to increase matrix synthesis and tissue formation over synthetic polymers.[81,103,112,113] While each individual biopolymer represents a single component of native articular cartilage, a more complete system, which includes a more comprehensive representation of native articular cartilage, is decellularized matrix. This matrix is obtained by proteolytically digesting cartilage from different animal sources and freeze drying it into an easy-to-use powder. A study by Kwon *et al.* used this method to harvest and prepare porcine articular cartilage and injected it subcutaneously into a mouse model.[114] By incorporating a fluorescently modified albumin protein, the matrix was shown to remain in place over time, which suggests that the material may stay localized if injected into a cartilage defect. These methods have also been used for meniscus repair,[115] which shows their efficacy as potentially therapeutic option for all chondral defects. Recently, decellularized matrix has also been modified with acrylate groups for photocrosslinking,[116] which helps to localize the matrix and slightly increases the mechanical integrity.

However, biopolymers do have significant limitations, mainly a lack of mechanical integrity. We have emphasized this point by compiling compression data on both synthetic and biopolymer hydrogels (Table 2) and compression data on human cartilage (Table 1). We conclude that many synthetic polymers have been optimized to meet a significant portion of the compression modulus range of native human cartilage, while most biopolymers fall short or can only meet the lower aspect of the normal human physiologic range. This deficit in biologic hydrogels has considerably limited the use of these materials and remains an area that requires further study.

Recent advances in hydrogel technologies have sought to combine synthetic and biological polymers to address the previously mentioned shortcomings. In theory, synthetic polymers provide initial mechanical properties and are further modified to exhibit signaling properties of biopolymers. Examples include cytokine containing microspheres, which have been imbedded into hydrogels to control the release of growth factors over time.[117–119] Others have modified growth factors to be conjugated directly to the polymer units of hydrogels, inducing long-term signaling *in vivo*. Place *et al.* modified the surface lysine residues of a TGF-β transporter protein with Trout's reagent and proceeded to conjugate this complex to free acrylate groups on PEG through Michael addition after the formation of a radical thiol.[120] TGF-β is then immobilized by its transport protein within a PEG gel, and released over a period of weeks. Lee *et al.* covalently bonded collagen-like mimetic peptides in conjunction with PEG to take advantage of the mechanical strength of PEG in addition to the signaling properties of collagen-like peptides.[113] These studies demonstrate the potential in combining several methods into one cohesive methodology to recapitulate many aspects of native cartilage. However, additional work must be done to refine the relationship between optimal mechanical strength and optimal biochemical signaling.

Hydrogels can be engineered into multilayered structures comprising of different polymers.[121,122] These advances demonstrate the potential in developing multiscale scaffolds, which integrate biological moieties and mechanical properties specific to each zone of cartilage within a single construct. In a two-part series by Nguyen *et al.*, it was shown that specific hydrogels can direct a single lineage of MSCs into zone-specific chondrocyte phenotypes.[121,122] To recapitulate the deep zone, PEG and HA were used, a combination of PEG and chondroitin sulfate was used for the middle zone; while the combination of PEG, chondroitin sulfate, and metalloprotease sensitive peptides were used for the superficial zone.[122] The hydrogel combinations resulted in an appropriate expression of markers for each zone; specifically type X collagen was found upregulated in the deep zone, while both type II collagen and proteoglycans were found to have moderate expression in the middle zone, and finally a high degree of type II collagen expression was found in the superficial zone.[122] In the second study by Nguyen *et al.*, these hydrogels were combined into a trilayered scaffold to demonstrate the ability to differentiate a single stem cell lineage into zone-specific chondrogenic phenotypes corresponding to all three zones of articular cartilage within a single construct.[121] As expected, the stacking of all three gels did successfully result in differentiation of MSCs into zone- specific chondrocyte phenotypes.[121] Recently Karimi *et al.* attempted a similar study, but used a modified PEG polymer with a compression modulus of 2.1 Mpa, which is closer to that of native articular cartilage.[123] Different concentrations and modified versions of acrylate-functionalized lactide-chain-extended polyethylene glycol (SPELA) were used to mimic each

Table 2. Mechanical Properties of Various Biologic and Synthetic Polymer Hydrogels from Previous Studies

Mechanical properties of hydrogels					
Hydrogel	*Author*	*Composition*	*Compressive test*	*Chemical alterations*	*Value (Kpa)*
Hyaluron	Burdick *et al.*[107]	350 kDa (5 wt%) HA, PBS	Young's	PEGDM:MAh	25 kPa
		50 kDa (5 wt%) HA, PBS			35 kPa
		50 kDa (20 wt%) HA, PBS			100 kPa
	Tan *et al.*[110]	1.25 wt% HA:CS (7:3), DPBS	Young's	PEGDA:thiol addition	12 kPa
		1.25 wt% HA:CS (5:5), DPBS			25 kPa
		1.25 wt% HA:CS (3:7), DPBS			28 kPa
	Jeon *et al.*[195]	1 wt% HA, PBS	Young's	PEG1000 (10%)	40 kPa
				PEG1000 (20%)	65 kPa
				PEG2000 (10%)	35 kPa
				PEG2000 (20%)	50 kPa
	Erickson *et al.*[83]	1 wt% HA, PBS	Compressive equilibrium	MAh	120 kPa
	Chung *et al.*[196]	1 wt% HA, PBS	Compressive equilibrium	MACL	55 kPa
	Chung *et al.*[197]	1 wt% HA, PBS	Compressive equilibrium	MAh	80 kPa
	Segura *et al.*[106]	3 wt% HA, PBS	Compressive modulus	PEGDG:biotin:collagen	33.5 kPa
	Nguyen *et al.*[122]	1 wt% HA, PBS	Compressive modulus	N/A	31.4 kPa
				PEG	330.6 kPa
				PEG:MMP-pep	184.28 kPa
				PEG:CS	74.02 kPa
				PEG:CS:MMP-pep	67.86 kPa
	Chung *et al.*[198]	1 wt% HA, PBS	Compressive modulus	MAh (7%) 2% photoinitiator: I2959	2.5 kPa
				MAh (7%) 5% photoinitiator: I2959	26.1 kPa
				MAh (12%) 2% photoinitiator: I2959	11.3 kPa
				MAh (12%) 20% photoinitiator: I2959	100.5 kPa
	Hwang *et al.*[199]	PEGDA:HA	Compressive modulus	Me photoinitiator: I2959	50.0 kPa
Chondroitin sulfate	Bryant *et al.*[104]	5% CS	Young's	MA (25%) photoinitiator: I2959	16 kPa
		10% CS			160 kPa
		20% CS			900 kPa
		30% CS			2600 kPa
		10% CS	Young's	MA (8%) photoinitiator: I2959	54 kPa
		20% CS			630 kPa
		30% CS			1200 kPa
		30% CS	Young's	MA (<1%) photoinitiator: I2959	10 kPa
	Nguyen *et al.*[122]	20% CS (w/v), PBS	Compressive modulus	N/A	82.39 kPa
		10% CS (w/v), PBS		PEG	117.80 kPa
		9% CS (w/v), PBS		PEG:MMP-pep photoinitiator: I2959	105.78 kPa
	Zhang *et al.*[112]	CS:HA (15:1) (w/w)	Young's	N/A	44.93 kPa
	Hwang *et al.*[199]	PEGDA:CS	Compressive modulus	MA photoinitiator: I2959	60.0 kPa
	Villanueva *et al.*[103]	PEGDM:CS-MA (8:2)	Young's	MA photoinitiator: I2959	78.0 kPa
		PEGDM:CS-MA (6:4)			70.0 kPa
	Strehin *et al.*[105]	CS-NHS:PEG (1:1)	Young's	pH 9.6	15 kPa
				pH 7.6	23 kPa
				pH 7.3 photoinitiator: TEA	30 kPa

(*continued*)

Table 2. (Continued)

Mechanical properties of hydrogels

Hydrogel	*Author*	*Composition*	*Compressive test*	*Chemical alterations*	*Value (Kpa)*
Poly(vinyl alcohol)	Holloway *et al.*[200]	20% PVA (w/w)	Unconfined compressive modulus	N/A	240 KPa
	Spiller *et al.*[201]	10% PVA (w/w)	Confined compressive modulus	PVP (1%)	111 KPa
Gelatin/collagen	Hwang *et al.*[199]	PEGDA:Col	Compressive modulus	MA photoinitiator: I2959	35.0 kPa
	Yu *et al.*[202]	Gel/HA:MAL-PEG-MAL (1:5)	Young's	Diels–Alder reaction	800 kPa
		Gel/HA:MAL-PEG-MAL (1:10)		MES buffer	1000 kPa
	Benton *et al.*[99]	GelMA (10% wt)	Young's	MA photoinitiator: I2959	42 kPa
	Hutson *et al.*[203]	GelMA (5%):PEGDMA (10%)	Young's	MA (20%) photoinitiator: I2959	35 kPa
		GelMA (10%):PEGDMA (10%)			40 kPa
		GelMA (15%):PEGDMA(10%)			80 kPa
PEG	Nguyen *et al.*[122]	20% PEG, PBS	Compressive modulus	N/A	293.21 kPa
	Villanueva *et al.*[103]	10% PEGDM	Young's	DMA (80%) photoinitiator: IHT-PI 659	60 kPa
		20% PEGDM			500 kPa
		30% PEGDM			900 kPa
	Nicodemus and Bryant [77]	10% PEGDM	Young's	DMA (90–95%) photoinitiator: IHT-PI 659	70 kPa
		20% PEGDM			600 kPa
	Bryant *et al.*[204]	10% PEGDM	Young's	Photoinitiator: I2959	34 kPa
		20% PEGDM			360 kPa

HA, hyaluronic acid; PBS, phosphate buffered saline; PEGDM, poly(ethylene glycol) dimethacrylate; PEGDMA, poly(ethylene glycol) dimethacrylate; MAh, methacrylic anhydride; CS, chondroitin sulfate; CS-NHS, chondroitin sulfate succinimidyl succinate; CS-MA, methacrylated chondroitin sulfate; PVA, poly(vinyl alcohol); MAL-PEG-MAL, dimaleimide poly(ethylene glycol); MES, 2-morpholinoethane sulfonic acid; PEG, poly(ethylene glycol); MA, methacrylated; DMA, dimethacrylate; IHT-PI 659, (1-[4-(2-hydroxyethoxy)-phenyl]-2-hydroxy-2-methyl-1-propane-1-one); DPBS, Dulbecco's phosphate buffered saline; PEGDA, poly(ethylene glycol) diacrylate; MACL, methacrylated caprolactone; MMP-pep, matrix metalloproteinase-sensitive peptides; TEA, triethanolamine; Col, type I collagen; GelMA, methacrylated gelatin; PEGDG, poly(ethylene glycol) digycidyl ether; I2959, 2-methyl-1-[4-(hydroxyethoxy)phenyl]-2-methyl-1-propanone.

zone. Fifteen percent of SPELA was used for the superficial zone, 50% SPELA was used for the middle zone, and a combination of PLA and SPELA 35% with HA was used for the deep zone.[123] This study also used TGFB1 in all three zones, but added BMP-7 to the superficial zone and IGF-1 to the middle zone. This study represents the first attempt to mimic the zonal composition of cartilage and the biochemical signaling of each zone in cartilage in a single study. A single cell lineage of human MSCs were encapsulated and allowed to differentiate. The superficial zone expressed type II collagen and SZP the most, which are superficial zone markers. The middle zone expressed moderate levels of all markers, while the deep zone expressed type X collagen and APL the most, consistent with deep zone markers.[123]

Despite the convenience and relative effectiveness of hydrogels as scaffolds for cartilage tissue engineering, many of these constructs still lack the mechanical properties to recapitulate the full range of normal articular cartilage (Table 1 and 2). Moreover, engineering hydrogels to increase their mechanical properties often comes at the expense of porosity. As previously mentioned, studies have shown that chondrocytes secrete less native matrix in denser hydrogels compared to porous gels and this can lead to poor tissue maturation and poor integration of engineered constructs *in vivo*.[78,80,124–129] Additionally, while hydrogels can interact with cells on a nanoscale, the actual nanoarchitecture of native cartilage has not been recapitulated by hydrogels. Great strides have been made to engineer hydrogels for cartilage tissue scaffolds; however, additional work to recapitulate the nanoarchitecture and improve mechanical strength may better address the current deficits observed in hydrogels.

Nanoengineering techniques: application to cartilage and future potential

Nanoscale approaches offer an integrative approach to synthetically engineered tissues. Capillary force lithography, nanoimprinting, two-photon lithography, SAPs, and electrospun nanofibers are common techniques used to engineer tissue architecture on a nanoscale.[130] Studies comparing micro and nanoscale topographical cues, from our group and others, have shown that a nanoscale approach provides the most reliable means to control cell fate and morphology.[130–134] In addition, many studies have also revealed the significance of mechanical signaling in relation to cell fate.[135–139] Striking a balance between a suitable biomaterial compatible with cell proliferation and mechanical stimulation while satisfying the nanoarchitectural parameters of a native tissue have become the forefront of tissue engineering. Cartilage physiology relies heavily on the properties resulting from collagen orientation, thus fibrogenesis and nanoscale architectures mimicking these orientations should be a priority for further research. Two techniques currently exist for replicating fibers at this length scale: electrospinning[140–145] and SAPs[146–149] (Fig. 3).

SAPs are small segments of amino acids, which self-assemble into nanoscale fibers. These fibers can be tuned to many different dimensions to meet a wide array of engineering criteria. Our group has demonstrated the therapeutic potential of SAPs, specifically KLD-12peptides, by showing their ability to reduce subchondral bone remodeling and protect implanted stem cells in a rat osteoarthritis model.[150] In spite of the apparent advantages for treating arthritis, the primary reason SAPs have not seen significant use in cartilage engineering is due to the lack of ability to control the extent of fiber assembly and orientation in cell-compatible material. Hairpin SAPs have shown some ability to organize by assembling into ordered betasheets, but the final hydrogel consists of disorganized macroassemblies of these sheets. Adler–Abramovich *et al.* developed a novel SAP fabrication method, which does succeed in controlling the final macrostructure orientation by using a phenylalanine vapor-deposition technique to create arrays of vertically oriented nanotubes (Fig. 3A, B).[149] However, this technique has yet to be used in cell culture, and thus its usefulness in the field of tissue engineering remains unknown. In spite of these limitations, SAPs can be administered through injection, which makes them desirable from a clinical translation standpoint.

Electrospinning offers a method to produce large numbers of micro and nanoscale fibers of varying compositions and in various orientations. Electrospinning has found considerable use for cartilage tissue engineering, in particular, for mimicking the superficial zone.[151,152] Collagen type I, collagen type II, polycaprolactone (PCL), and many other synthetic polymer nanofibers have been electrospun to mimic aspects of native cartilage.[140–145,153–159] Baker and Mauck showed that nanofiber alignment does have an effect on scaffold mechanical properties.[160] In this study, the fiber alignment allowed for a 63% increase in tensile strength over 70 days of culture to a modulus approaching 19.7 MPa. Nanofibers have also demonstrated the ability to direct cell differentiation down the chondrocyte lineage.[161,151] PCL nanofibers have been used to differentiate MSCs, in the presence of TGF-β, which led to a chondrocyte phenotype.[161] Human MSCs were cultured in chondrogenic media on PCL nanofiber scaffolds and differentiated into chondrocyte lineages.[151] Another advantage is the added control over fiber orientation. A study by McCullen *et al.* created a 1 mm tall trilayered nanofiber scaffold simply by changing the electrospinning parameters at regular intervals.[162] The resulting construct loosely resembled the collagen architecture of native articular cartilage. These studies exemplify the potential of nanofibers to enhance cartilage tissue engineering as a means to recapitulate the organization of the native ECM as well as to drive cellular differentiation while providing initial mechanical properties that can withstand *in vivo* mechanical loading parameters.

Advances in nanofiber fabrication have focused on the development of surface functionalization to improve the biocompatibility and bioreactivity of nanofibrous scaffolds.[163] A review by Sang Yoo *et al.* summarizes these major techniques.[163] Briefly, plasma treatment, surface graft polymerization, wet chemical method, and bioactive molecule immobilization have all been used to functionalize nanofibers.[163] Stendahl functionalized nanofibers with vascular endothelial growth factor (VEGF) and fibroblast growth factor (FGF) through heparin–polymer interactions.[164] By utilizing heparin-binding peptide amphiphiles, nanofibers were formed first with the introduction of heparin and then subsequently functionalized with VEGF and FGF and introduced into mouse omentum. The VEGF- and FGF-functionalized nanofibers significantly increased blood vessel density in comparison to the nonfunctionalized nanofiber

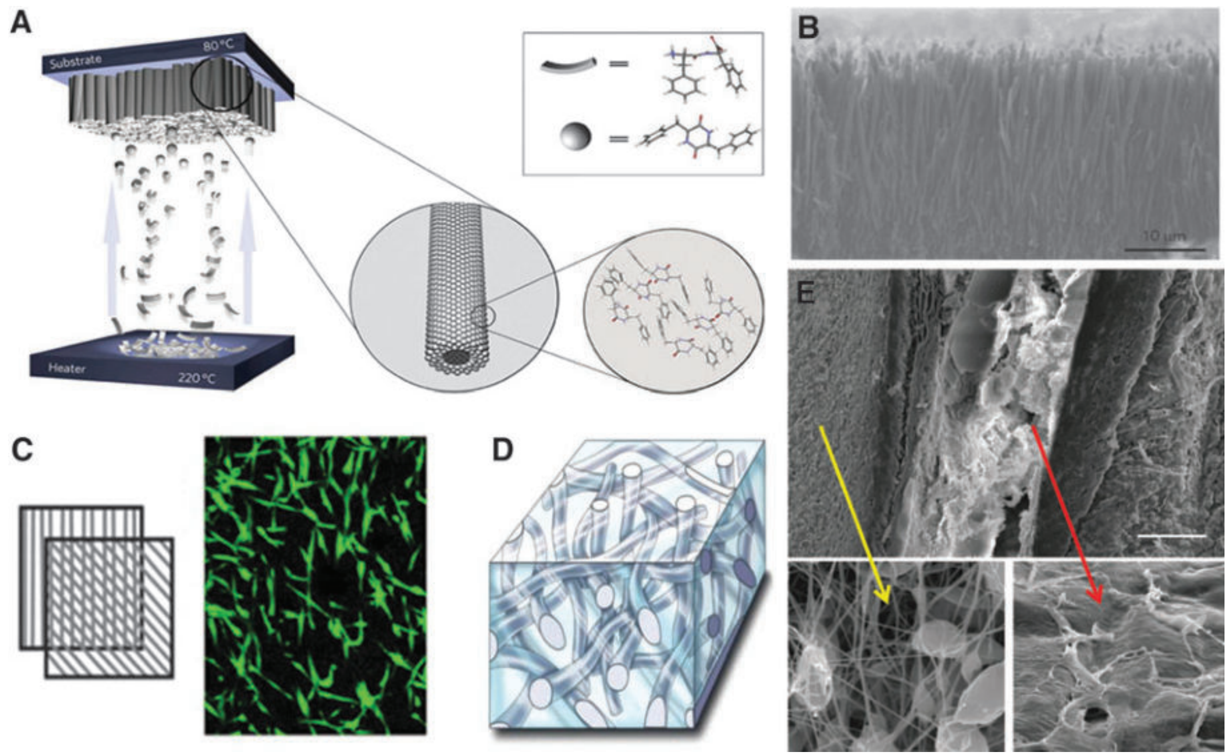

FIG. 3. Nanoengineering techniques used to recapitulate extracellular matrix (ECM) architecture. **(A)** Illustration of phenylalanine nanotubes fabricated using a vapor deposition technique, assembled into arrays of nanotubes.[146] **(B)** SEM image of the phenylalanine vertically oriented nanotube arrays.[146] **(C)** Through their submersion in a hydrogel, fiber sheets can also be oriented in space.[161] **(D)** An illustration demonstrating a hydrogel–nanofiber hybrid scaffold, which can be generated by electrospinning nanofibers onto a hydrogel.[164] **(E)** SEM image of cell suspension–hydrogel layers in combination with nanofiber sheets created by modifying an inkjet printer head to deposit hydrogel–cell suspension in tandem with the deposition of electrospun fibers.[166] SEM, scanning electron microscopy.

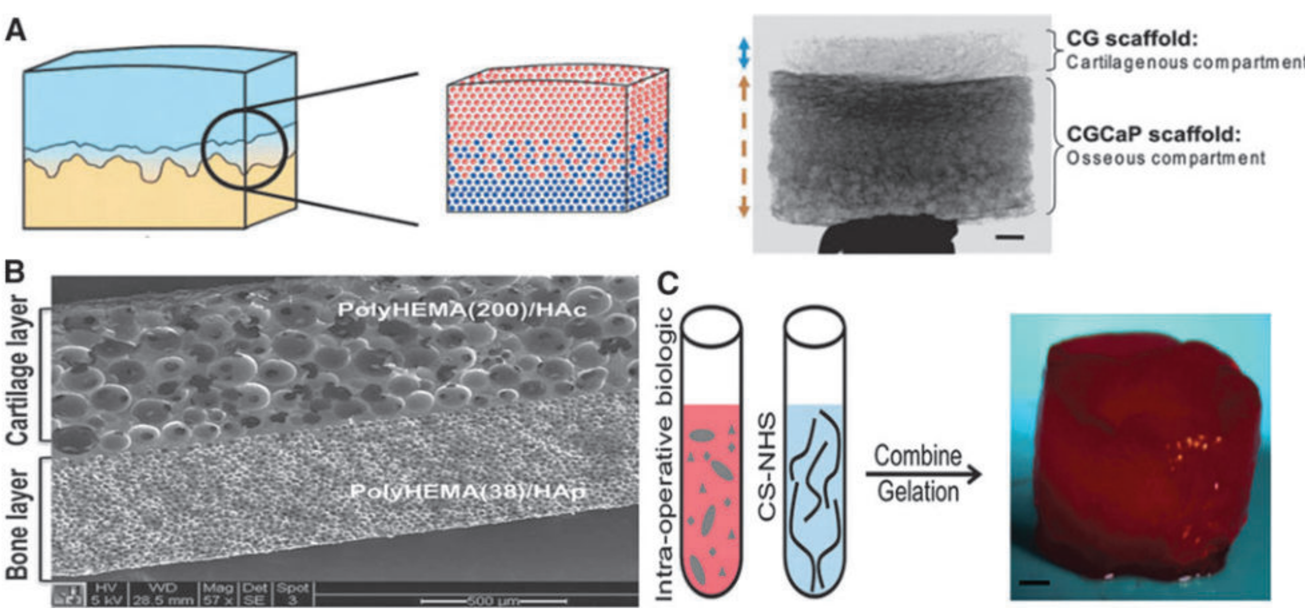

FIG. 4. Nanoengineering techniques used to fabricate osteochondral bilayers. **(A)** Illustration demonstrating how liquid cosynthesis is used to form the transition between bone and cartilage.[174] **(B)** SEM image showing dissolvable nanoparticles submerged in polymer to create two separate zones within a single scaffold.[176] **(C)** Illustration and image of bioadhesive synthesis from native ECM molecules such as chondroitin sulfate succinimidyl succinate (CS-NHS) and further enhanced with the addition of platelet-rich plasma to stimulate matrix synthesis.[179]

control group, thus demonstrating the ability to localize growth factors to nanofibers to enhance tissue formation. Kim *et al.* coelectrospun HA and collagen-functionalized nanofibers through a sodium hydroxide/N,N-dimethyl formamide mixture.[165] When these hybrid scaffolds were seeded with bovine joint chondrocytes *in vitro*, the results indicated a 4.5-fold increase in cell number on HA/collagen scaffolds over HA only scaffolds after a 7-day culture period.[165] This functionalization demonstrates the ability to localize important ECM proteins onto nanofibers, which allows a synthetic polymer to stimulate cells both architecturally and by recapitulating native ECM signaling interactions.

Another innovative use for nanofibers is their incorporation into hydrogels. Yang *et al.* 2011 utilized nanofibers suspended within hydrogels to demonstrate that cells could be organized into three-dimensional spaces, and organized as independent sheets (Fig. 3C).[166] This study shows that nanofibers can be used to recapitulate nanoscale architecture within a hydrogel. Additional studies have utilized ground nanofibers, or short segments, as scaffolding support in hydrogels.[167–169] This method is analogous to the way in which reinforcing steel bars (rebar) are used in concrete to improve its overall mechanical strength. The result of nanofiber-reinforced hydrogels has produced a strength increase by an entire order of magnitude.[168,205] Colburn *et al.* developed a similar approach by using a hydrogel solution as the collecting plate for PCL nanofibers, thus creating a random 3D homogeneous mixture of uncut nanofibers and hydrogel (Fig. 3D),[170] closely resembling the collagen structure of the middle zone of native articular cartilage. The application of nanofiber hydrogel constructs has been a recent development, but these early studies have only begun to expose the power of a hybrid approach.

Taking this hybrid fabrication technique further, other investigators have utilized rapid prototyping to print cells in a 3D arrangement of choice within a hydrogel matrix. Moroni *et al.* combined the approaches of electrospinning with rapid prototyping technology to create a system that layers nanofibers and hydrogels into thick constructs.[171] Shim *et al.* used rapid prototyping technology to print biomaterials, which incorporate both signaling factors into hydrogels in a three-dimensional structure.[172] Tao *et al.* further advanced this technology by utilizing a system similar to the bioplotter to print a cell suspension into a nanofiber and hydrogel scaffold (Fig. 3E).[173] The combined technology developed by Tao allows for a layer of nanofibers to be electrospun onto a layer of hydrogel with encapsulated cells, but the nanofibers lack organization and the overall tissue construct does not fully recapitulate the native architecture of cartilage. Many of the pitfalls associated with hydrogels have been addressed in rapid prototyping systems. Levato *et al.* increased the compression modulus of a gelatin hydrogel for bone tissue engineering by seeding MSCs in PLA microcarriers.[174] Another study by Shim *et al.* printed two separate cell phenotypes in the same scaffold to create an osteochondral tissue with enhanced mechanical properties, but also allowed for a three-dimensional arrangement of two cell phenotypes in an anatomically relevant structure.[175]

Through the combination of many techniques, progress has been made to improve the zonal architecture of articular cartilage scaffolds, the mechanical properties of these scaffolds, and the ability to recapitulate native cartilage ECM and growth factor signaling. These studies represent the state of the art in cartilage engineering, and continued development will hopefully result in a single scaffold design, which allows all aspects of articular cartilage to be replicated. It is worthy to note that the successes highlighted in this review stem from novel combinations of fabrication techniques, which interact with stem cells or chondrocytes on a nanoscale, molecular scale, and microscale, thus emphasizing the need for continued effort toward developing multiscale engineering methods.

Engineering the transition zone

Integrating engineered tissues into host models is a long standing challenge in many areas of tissue engineering. Early studies into hydrogels found that constructs often dissolved and disappeared from sites of implantation or the scaffold failed to integrate.[125–129,176] The problem of implant integration has birthed a new area of research dedicated to solving this problem. bioglue, hybrid gels, and multilayered constructs have all been pursued as viable solutions (Fig. 4). Many studies have tried to address this problem by engineering the transition zone between bone and cartilage into a single construct.

Lessons learned from limb development and chondrogenesis can serve as guiding parameters for engineering the transition zone. By understanding chondrogenesis, the possibility exists to differentiate a single stem cell line into two separate tissues of bone and cartilage. Mature bone is primarily comprised of type I collagen and organic phosphates in the form of hydroxyapatite.[177–179] Mature articular cartilage is comprised of type II collagen, aggrecan, and rich in HA and keratin sulfate. These simple differences may be sufficient to differentiate stem cells into two separate lineages. We have shown that the presence of HA bound to a dopamine functionalized nanopattern was sufficient to drive dental pulp stem cells to a chondrocyte lineage.[180] In the same study, BMP-4 was also utilized, and encouraged a hypertrophic morphology reminiscent of chondrocytes in the stages before ossification. Another study by Mouthuy *et al.* utilized PLGA nanofibers with hydroxyapatite and type I collagen to mimic bone.[181] When the nanofibers were layered with MSC sheets and cultured in a chondrogenic media, the combined stimuli resulted in MSC differentiation into a transition zone phenotype, supported by the presence of type X collagen. While neither of these studies developed a full osteochondral bilayer scaffold, each study succeeded in applying knowledge of biology of the native transition zone and chondrogenic growth factors to replicate an element of that zone from stem cells.

Other studies have utilized multilayered scaffolds in an effort to produce a unified transition tissue (Fig. 4). A common approach, and one that has seen some clinical use, entails the use of compressed collagen to make a porous sponge. The method briefly: create a solution of the desired collagen type and ECM components, freeze dry it, then add the next layer and repeat. The typical pore size produced in these methods ranges from 150 to 400 μm, which allows for ample cell migration. Qi *et al.* utilized this method to implant a homogeneous compressed type I collagen scaffold into a rabbit model and showed good integration of the scaffold.[182] Harley *et al.* elaborated on the sponge method by using unique mixtures for each zone (Fig. 4A).[183] By freeze drying the solutions through liquid phase cosynthesis, Harley successfully created a gradient between the mixtures similar to a transition zone.[183] Yunos *et al.*also created a bilayered scaffold by attaching poly-DL-lactide (PDLLA) nanofibers to bioglass ceramic, which supported chondrocyte cell proliferation in culture.[184] Another recent study by Galperin *et al.* utilized dissolvable nanoparticles, coated with either HA or hydroxyapatite, submerged in polymer to create two different zones. This bilayer scaffold showed MSC differentiation into both cartilage and bone without the need for growth factors (Fig. 4B).[185]

Collagen sponges, and similar scaffolding, have been used in small clinical studies and been shown to have efficacy as a potential alternative to patients who qualify for microfracture procedures, which is the current standard of care for patients with relatively small cartilage defects. A study by Efe *et al.* implanted a collagen type 1 sponge into 15 patients with articular cartilage defects less than 11 mm in diameter.[186] Preoperative and 1 year postoperative International Knee Documentation Committee (IKDC) scores were taken. The patients experienced significant improvement in their IKDC scores, denoted by an increase from an average of 48 preoperative to $\sim$70 one year postoperative. A larger series with 116 patients by Schneider *et al.* implanted a product called The Cartilage Regeneration System (CaReS), which is a type I collagen hydrogel seeded with autologous chondrocytes.[187] The average cartilage defect was 5.4 cm^2, and almost every patient reported an improved IKDC score. The average preoperative score was 42.4, with a statistically significant improvement at 2 years postoperative with an average score of 70.5. A study by Stanish *et al.* used a novel chitosan-based acellular sponge (BST-CalCell) to treat 41 patients.[188] In comparison to 39 patients who received a microfracture procedure, the BST group had significantly more lesion filling and articular cartilage at 1 year based on magnetic resonance imaging studies. One pitfall of these studies is a lack of transition from cartilage to bone to enhance scaffold integration. A study by Filardo *et al.* used a three-layered scaffold comprising of a gradient between hydroxyapatite and collagen 1 to treat 27 patients.[189] The average defect was 3.4 cm^2, and the average preoperative IKDC score was 40. At 1 year, the average IKDC had risen to 85, which is the largest increase of IKDC score compared to the previously discussed studies. This study suggests that implanting an osteochondral scaffold has more benefit to the patient than a cartilage scaffold alone. Larger clinical trials are needed to confirm these results, but this early data are encouraging. Moreover, this provides evidence to support the need to continue to engineer each zone of articular cartilage, including the transition zone, for the purpose of improving patient outcome.

Another approach for securing cartilage implants is bioglue. This method may circumvent the need to engineer a transition between cartilage and bone by sufficiently securing a cartilage scaffold to bone, or may offer a way to secure bone to bone-cartilage transition scaffolds. In general bioglues are pivotal solutions to the issue of implantation. In the context of cartilage, two studies have been conducted with promising results. Wang *et al.*, created a novel bioglue derived from methacrylated chondroitin sulfate, which readily bonds to bone and cartilage as well as hydrogels.[190] One of the most novel aspects of this material is the presence of photoreactive groups, which allows for instant curing using UV light. This material had been further developed to include platelet-rich plasma (PRP) in the bioglue solution (Fig. 4C).[191] PRP has become a popular injection therapy for degrading articular joints due to the presence of growth factors within PRP that have been implicated in chondrogenesis.[192] The inclusion of PRP into a chondroitin bioglue allows the bioglue to act as an adhesive in addition to providing both ECM signaling and growth factor signaling, which improves tissue integration into native skeletal tissues over other bioadhesives.

Conclusion and future perspective

Cartilage tissue engineering has evolved over many years from simple scaffolds and basic cell suspensions to complex multilayered systems. This review has described many of the techniques being employed to regenerate human articular cartilage and we have tried to emphasize methods that utilize a multiscale engineering approach.

While many of these methods have yielded individual elements of cartilage, few studies have investigated a more cohesive methodology, by combining techniques to recapitulate the entire depth of the native cartilage, especially with regard to the zone-specific organization of the collagen fibers of the matrix. We believe that a multiscale bioengineering approach, taking into account these features, may be an important direction for future work and may lead to more successful tissue generation. By integrating nanoengineering techniques, which have shown promise in directing cellular processes more accurately, functional tissue generation may be improved. This may represent a more anatomic articular cartilage replacement in the future, which will have a tremendous clinical impact if it can be applied to the innumerable patients with cartilage injury and arthritis.

Acknowledgments

This work was supported by the Departments of Bioengineering and Orthopedics and Sports Medicine at the University of Washington. Additional support was provided by the Mary Gates Research Scholarship at the University of Washington. The authors thank James Dennis for critical reading of this article.

Disclosure Statement

No competing financial interests exist.

References

1. Weiss, C., Rosenberg, L., and Helfet, A. An ultrastructural study of normal young adult human articular cartilage. J Bone Joint Surg Am **50,** 663, 1968.
2. Roughley, P., and Lee, E. Cartilage proteoglycans: structure and potential functions. Microsc Res Tech **28,** 385, 1994.
3. Poole, C., and Flint, M. Chondrons in cartilage: ultrastructural analysis of the pericellular microenvironment in adult human articular cartilages. J Orthop Res **5,** 509, 1987.
4. Hunziker, E., Quinn, T., and Häuselmann, H. Quantitative structural organization of normal adult human articular cartilage. Osteoarthritis Cartilage **10,** 564, 2002.

5. Matukas, V., Panner, B., and Orbison, J. Studies on ultrastructural identification and distribution of protein-polysaccharide in cartilage matrix. J Cell Biol **32,** 365, 1967.
6. Hall, A., Horwitz, E., and Wilkins, R. The cellular physiology of articular cartilage. Exp Physiol **81,** 535, 1996.
7. Frank, E., and Grodzinsky, A. Cartilage electromechanics—I. Electrokinetic transduction and the effects of electrolyte pH and ionic strength. J Biomech **20,** 615, 1987.
8. Park, S., Krishnan, R., Nicoll, S., and Ateshian, G. Cartilage interstitial fluid load support in unconfined compression. J Biomech **36,** 1785, 2003.
9. Xia, Y., Farquhar, T., and Burton-Wurster, N. Diffusion and relaxation mapping of cartilage-bone plugs and excised disks using microscopic magnetic resonance imaging. Magn Reson Med **31,** 273, 1994.
10. Burstein, D., Gray, M., and Hartman, A.L. Diffusion of small solutes in cartilage as measured by nuclear magnetic resonance (NMR) spectroscopy and imaging. J Orthop Res **11,** 465, 1993.
11. Maroudas, A. Distribution and diffusion of solutes in articular cartilage. Biophys J **10,** 365, 1970.
12. Zizak, I., Roschger, P., Paris, O., and Misof, B. Characteristics of mineral particles in the human bone/cartilage interface. J Struct Biol **141,** 208, 2003.
13. Quinn, T., Dierickx, P., and Grodzinsky, A. Glycosaminoglycan network geometry may contribute to anisotropic hydraulic permeability in cartilage under compression. J Biomech **34,** 1483, 2001.
14. Mow, C., Proctor, C., and Kelly, M. Biomechanics of articular cartilage. In: Nordin, M., and Frankely, VH., eds. Basic biomechanics of the musculoskeletal system. Philadelphia: Lea & Febiger, 1989, pp. 31–58.
15. Blanco, F., Guitian, R., and Vázquez-Martul, E. Osteoarthritis chondrocytes die by apoptosis: a possible pathway for osteoarthritis pathology. Arthritis Rheum **41,** 284, 2004.
16. Helmick, C., Atlanta, G., Felson, D., Boston, M., and Lawrence, R. Estimates of the prevalence of arthritis and other rheumatic conditions in the United States. Part I. Arthritis Rheum **58,** 15, 2008.
17. Bijlsma, J., Berenbaum, F., and Lafeber, F. Osteoarthritis: an update with relevance for clinical practice. Lancet **377,** 2115, 2011.
18. Francetti, L., Azzola, F., Corbella, S., Taschieri, S., and Fabbro, M. Evaluation of clinical outcomes and bone loss around titanium implants with oxidized surface: six-year follow-up results from a prospective case series study. Clin Implant Dent Relat Res **16,** 81, 2014.
19. Fontaine, K., Haaz, S., and Heo, M. Projected prevalence of US adults with self-reported doctor-diagnosed arthritis, 2005 to 2050. Clin Rheumatol **26,** 772, 2007.
20. Hootman, J., and Helmick, C. Projections of US prevalence of arthritis and associated activity limitations. Arthritis Rheum **54,** 226, 2005.
21. Gravallese, E. Bone destruction in arthritis. Ann Rheum Dis **2,** 84, 2002.
22. Walsh, N., and Gravallese, E. Bone remodeling in rheumatic disease: a question of balance. Immunol Rev **233,** 301, 2010.
23. Wesolowski, G., Mclane, J., and Bone, A. The role of subchondral bone remodeling in osteoarthritis: reduction of cartilage degeneration and prevention of osteophyte formation by alendronate in the in the rat anterior cruciate ligament transection model. Arthritis Rheum **50,** 1193, 2004.
24. Hashimoto, S., and Creighton-Achermann, L. Development and regulation of osteophyte formation during experimental osteoarthritis. Osteoarthritis Cartilage **10,** 180, 2002.
25. Wu, Z., Nagata, K., and Iijima, T. Involvement of sensory nerves and immune cells in osteophyte formation in the ankle joint of adjuvant arthritic rats. Histochem Cell Biol **118,** 213, 2002.
26. Ho, A., Johnson, M., and Kingsley, D. Role of the mouse ank gene in control of tissue calcification and arthritis. Science **289,** 265, 2000.
27. Koenders, M., Lubberts, E., and Oppers-Walgreen, B. Blocking of interleukin-17 during reactivation of experimental arthritis prevents joint inflammation and bone erosion by decreasing RANKL and interleukin-1. Am J Pathol **167,** 141, 2005.
28. Lubberts, E., and van den Bersselaar, L. IL-17 promotes bone erosion in murine collagen-induced arthritis through loss of the receptor activator of NF-κB ligand/osteoprotegerin balance. J Immunol **170,** 2655, 2003.
29. Gravallese, E., Harada, Y., and Wang, J. Identification of cell types responsible for bone resorption in rheumatoid arthritis and juvenile rheumatoid arthritis. Am J Pathol **152,** 943, 1998.
30. Klein, T., Malda, J., Sah, L., and, Hutmacher, W. Tissue engineering of articular cartilage with biomimetic zones. Tissue Eng Part B Rev **15,** 143, 2009.
31. Elisseeff, J., and Sharma, B. Engineering structurally organized cartilage and bone tissues. Ann Biomed Eng **32,** 148, 2004.
32. Venn, M., and Maroudas, A. Chemical composition and swelling of normal and osteoarthrotic femoral head cartilage. I. Chemical composition. Ann Rheum Dis **36,** 121, 1977.
33. Eyre, D. Collagen of articular cartilage. Arthritis Res **4,** 30, 2002.
34. Cohen, N., Foster, R., and Mow, V. Composition and dynamics of articular cartilage: structure, function, and maintaining healthy state. J Orthop Sports Phys Ther **28,** 203, 1998.
35. Schmidt, T., Gastelum, N., and Nguyen, Q. Boundary lubrication of articular cartilage: role of synovial fluid constituents. Arthritis Rheum **56,** 882, 2007.
36. Nugent-Derfus, G., and Chan, A. PRG4 exchange between the articular cartilage surface and synovial fluid. J Orhop Res **25,** 1269, 2007.
37. Ikegawa, S., Sano, M., and Koshizuka, Y. Isolation, characterization and mapping of the mouse and human PRG4 (proteoglycan 4) genes. Cytogenet Cell Genet **90,** 291, 2000.
38. Malda, J., Hoope, W., and Schuurman, W. Localization of the potential zonal marker clusterin in native cartilage and in tissue-engineered constructs. Tissue Eng Part A **16,** 897, 2009.
39. Watanabe, H., Yamada, Y., and Kimata, K. Roles of aggrecan, a large chondroitin sulfate proteoglycan, in cartilage structure and function. J Biochem **124,** 687, 1998.
40. Knudson, C., and Knudson, W. Cartilage proteoglycans. Cell Dev Biol **12,** 69, 2001.
41. Sekiya, I., Tsuji, K., Koopman, P., and Watanabe, H. SOX9 enhances aggrecan gene promoter/enhancer activity and is up-regulated by retinoic acid in a cartilage-derived cell line, TC6. J Biol Chem **275,** 10738, 2000.

42. Struglics, A., Larsson, S., Pratta, M., and Kumar, S. Human osteoarthritis synovial fluid and joint cartilage contain both aggrecanase-and matrix metalloproteinase-generated aggrecan fragments. Osteoarthritis Cartilage **14,** 101, 2006.
43. Flugge, L., Miller-Deist, L., and Petillo, P. Towards a molecular understanding of arthritis. Chem Biol **6,** 157, 1999.
44. Bollet, A., Handy, J., and Sturgill, B. Chondroitin sulfate concentration and protein-polysaccharide composition of articular cartilage in osteoarthritis. J Clin Invest **42,** 853, 1963.
45. Chan, P., Caron, J., Rosa, G., and Orth, M. Glucosamine and chondroitin sulfate regulate gene expression and synthesis of nitric oxide and prostaglandin E 2 in articular cartilage explants. Osteoarthritis Cartilage **13,** 387, 2005.
46. Holmes, M., Bayliss, M., and Muir, H. Hyaluronic acid in human articular cartilage. Age-related changes in content and size. Biochem J **250,** 435, 1988.
47. Fukuda, K., Dan, H., Takayama, M., and Kumano, F. Hyaluronic acid increases proteoglycan synthesis in bovine articular cartilage in the presence of interleukin-1. J Pharmacol Exp Ther **277,** 1672, 1996.
48. Chung, C., and Burdick, A. Engineering cartilage tissue. Adv Drug Deliv rev **60,** 243, 2008.
49. Eberhardt, A., Keer, L., and Lewis, J. An analytical model of joint contact. J Biomech Eng **112,** 407, 1990.
50. Smith, R., Trindade, M., Ikenoue, T., and Mohtai, M. Effects of shear stress on articular chondrocyte metabolism. Biorheology **37,** 95, 2000.
51. Lee, M., Trindade, M., Ikenoue, T. Effects of shear stress on nitric oxide and matrix protein gene expression in human osteoarthritic chondrocytes in vitro. J Orthop Res **20,** 556, 2002.
52. Williamson, A., Chen, A., and Sah, R. Compressive properties and function–composition relationships of developing bovine articular cartilage. J Orthop Res **19,** 1113, 2001.
53. Mendler, M., Eich-Bender, S., and Vaughan, L. Cartilage contains mixed fibrils of collagen types II, IX, and XI. J Cell Biol **108,** 191, 1989.
54. Gleghorn, J., Jones, A., and Flannery, C. Boundary mode lubrication of articular cartilage by recombinant human lubricin. J Orthop Res **27,** 771, 2009.
55. Hasty, K., Reife, R., and Kang, A. The role of stromelysin in the cartilage destruction that accompanies inflammatory arthritis. Arthritis Rhem **33,** 388, 2005.
56. Mahmoudifar, N., and Doran, M. Chondrogenesis and cartilage tissue engineering: the longer road to technology development. Trends Biotechnol **30,** 166, 2012.
57. Glowacki, J., Trepman, E., and Folkman, J. Cell shape and phenotypic expression in chondrocytes. Proc Soc Exp Biol Med **172,** 93, 1983.
58. Aydelotte, M., and Kuettner, K. Differences between subpopulations of cultured bovine articular chondrocytes. I. Morphology and cartilage matrix production. Connect Tissue Res **18,** 205, 1988.
59. Gerstenfeld, L., Kelly, C., and Deck, M. Comparative morphological and biochemical analysis of hypertrophic, non-hypertrophic and l, 25 (OH) 2D3 treated non-hypertrophic chondrocytes. Connect Tissue Res **24,** 29, 1990.
60. Chen, A., Bae, W., Schinagl, R., and Sah, R. Depth- and strain-dependent mechanical and electromechanical properties of full-thickness bovine articular cartilage in confined compression. J Biomech **34,** 1, 2001.
61. Oettmeier, R., and Abendroth, K. Analyses of the tidemark on human femoral heads. II. Tidemark changes in osteoarthrosis—a histological and histomorphometric study in non-decalcified preparations. Acta Morphol Hun **37,** 169, 1989.
62. Redler, I., Mow, V., Zimny, M., and Mansell, J. The ultrastructure and biomechanical significance of the tidemark of articular cartilage. Clin Orthop Relat Res **112,** 357, 1975.
63. Poole, C., Flint, M., and Beaumont, B. Morphological and functional interrelationships of articular cartilage matrices. J Anat **138,** 113, 1984.
64. Otsuki, S., Hanson, R., Miyaki, S., Grogan, P., Kinoshita, M., and Asaharam H. Extracellular sulfatases support cartilage homeostasis by regulating BMP and FGF signaling pathways. Proc Natl Acad Sci U S A **107,** 10202, 2010.
65. Goldring, M., and Marcu, K. Cartilage homeostasis in health and rheumatic diseases. Arthritis Res Ther **11,** 224, 2009.
66. Hashimoto,M,. Nakasa, T., and Hikata T. Molecular network of cartilage homeostasis and osteoarthritis. Med Res Rev **28,** 464, 2008.
67. Treppo, S., Koepp, H., Quan, E., and Cole, A. Comparison of biomechanical and biochemical properties of cartilage from human knee and ankle pairs. J Orthop Res **18,** 739, 2000.
68. Shepherd, D., and Seedhom, B. The''instantaneous'' compressive modulus of human articular cartilage in joints of the lower limb. Rheumatology (Oxford) **38,** 124, 1999.
69. Kurkijärvi, J., Nissi, M., and Kiviranta, I. Delayed gadolinium-enhanced MRI of cartilage (dGEMRIC) and T2 characteristics of human knee articular cartilage: topographical variation and relationships to mechanical properties. Magn Reson Med **52,** 41, 2004.
70. Huang, C., Stankiewicz, A., and Ateshian, G. Anisotropy, inhomogeneity, and tension–compression nonlinearity of human glenohumeral cartilage in finite deformation. J Biomech **38,** 799, 2005.
71. Chen, S., Falcovitz, Y., and Schneiderman, R. Depth-dependent compressive properties of normal aged human femoral head articular cartilage: relationship to fixed charge density. Osteoarthritis Cartilage **9,** 561, 2001.
72. Barker, M., and Seedhom, B. The relationship of the compressive modulus of articular cartilage with its deformation response to cyclic loading: does cartilage optimize its modulus so as to minimize the strains arising in it due to the prevalent loading regime? Rheumatology (Oxford) **40,** 274, 2001.
73. Raeber, P., Lutolf, P., and Hubbell, A. Molecularly engineered PEG hydrogels: a novel model system for proteolytically mediated cell migration. Biophys J **89,** 1374, 2005.
74. Friedl, P., and Wolf, K. Plasticity of cell migration: a multiscale tuning model. J Cell Biol **188,** 11, 2010.
75. Zeng, L., Yao, Y., Wang, D., and Chen, X. Effect of microcavitary alginate hydrogel with different pore sizes on chondrocyte culture for cartilage tissue engineering. Mater Sci Eng C Mater Biol Appl **34,** 168, 2014.
76. Nicodemus, D., Skaalure, C., and Bryant J. Gel structure has an impact on pericellular and extracellular matrix

deposition, which subsequently alters metabolic activities in chondrocyte-laden PEG hydrogels. Acta Biomater **7,** 492, 2011.
77. Nicodemus, G., and Bryant, S. The role of hydrogel structure and dynamic loading on chondrocyte gene expression and matrix formation. J Biomech **41,** 1528, 2008.
78. Bryant, S., and Anseth, K. Controlling the spatial distribution of ECM components in degradable PEG hydrogels for tissue engineering cartilage. J Biomed Mater Res A **64,** 70, 2003.
79. Bryant, S., Nicodemus, G., and Villanueva, I. Designing 3D photopolymer hydrogels to regulate biomechanical cues and tissue growth for cartilage tissue engineering. Pharm Res **10,** 2379, 2008.
80. Bryant, S., Anseth, K., and Da, L. Crosslinking density influences the morphology of chondrocytes photoencapsulated in PEG hydrogels during the application of compressive strain. J Orthop Res **22,** 1143, 2004.
81. Chung, C., and Burdick, J. Influence of three-dimensional hyaluronic acid microenvironments on mesenchymal stem cell chondrogenesis. Tissue Eng Part A **15,** 243, 2008.
82. Guvendiren, M., and Burdick, J. The control of stem cell morphology and differentiation by hydrogel surface wrinkles. Biomaterials **31,** 6511, 2010.
83. Erickson, E., Huang, H., Sengupta, S., Kestle, S., Burdick, A., and Mauck, L. Macromer density influences mesenchymal stem cell chondrogenesis and maturation in photocrosslinked hyaluronic acid hydrogels. Osteoarthritis Cartilage **17,** 1639, 2009.
84. Matsiko, A., Gleeson, P., and O'Brien, J. Scaffold mean pore size influences mesenchymal stem cell chondrogenic differentiation and matrix deposition. Tissue Eng Part A **21,** 486, 2015.
85. Bryant, S., Bender, R., and Durand, K. Encapsulating chondrocytes in degrading PEG hydrogels with high modulus: engineering gel structural changes to facilitate cartilaginous tissue production. Biotechnol Bioeng **86,** 747, 2004.
86. Weber, M., Lopez, G., and Anseth, S. Effects of PEG hydrogel crosslinking density on protein diffusion and encapsulated islet survival and function. J Biomed Mater Res A **90,** 720, 2009.
87. Engberg, K., and Frank, W. Protein diffusion in photopolymerized poly(ethylene glycol) hydrogel networks. Biomed Mater **6,** 5, 2011.
88. Ladet, G., Tahiri, K., Montembault, S., Domard, J., and Corvol, M. Multi-membrane chitosan hydrogels as chondrocytic cell bioreactors. Biomaterials **32,** 5354, 2011.
89. Park, M., Chun, C., Cho, C., and Song, S. Enhancement of sustained and controlled protein release using polyelectrolyte complex-loaded injectable and thermosensitive hydrogel. Eur J Pharm Biopharm **76,** 179, 2010.
90. Koutsopoulos, S., Unsworth, D., Nagai, Y., and Zhang, S. Controlled release of functional proteins through designer self-assembling peptide nanofiber hydrogel scaffold. Proc Natl Acad Sci U S A **106,** 4623, 2009.
91. Sutter, M., Siepmann, J., Hennink, E., and Jiskoot, W. Recombinant gelatin hydrogels for the sustained release of proteins. J Control Release **119,** 301, 2007.
92. Fiedler, J., Brill, C., Blum, W., and Brenner, R. IGF-I and IGF-II stimulate directed cell migration of bone-marrow-derived human mesenchymal progenitor cells. Biochem Biophys Res Commun **345,** 1177, 2006.
93. Fortier, L., Mohammed, H., and Lust G. Insulin-like growth factor-I enhances cell-based repair of articular cartilage. J Bone Joint Surg Br **84,** 276, 2002.
94. Huang, Q., Goh, J., and Hutmacher, D. In vivo mesenchymal cell recruitment by a scaffold loaded with transforming growth factor β 1 and the potential for in situ chondrogenesis. Tissue Eng **8,** 469, 2002.
95. Lin, H., Cheng, W., Alexander, G., Beck, M., and Tuan, S. Cartilage tissue engineering application of injectable gelatin hydrogel with in situ visible-light-activated gelation capability in both air and aqueous solution. Tissue Eng Part A **20,** 2402, 2014.
96. Hoshikawa, A., Nakayama, Y., Matsuda, T., Oda, H., Nakamura, K., and Mabuchi, K. Encapsulation of chondrocytes in photopolymerizable styrenated gelatin for cartilage tissue engineering. Tissue Eng **12,** 2333, 2006.
97. Visser, J., Gawlitta, D., Benders, M., Toma, H., Pouran, B., and van Weeren, R. Endochondral bone formation in gelatin methacrylamide hydrogel with embedded cartilage-derived matrix particles. Biomaterials **37,** 174, 2015.
98. Hu, X., Ma, L., Wang, C., and Gao, C. Gelatin hydrogel prepared by photo-initiated polymerization and loaded with TGF-beta1 for cartilage tissue engineering. Macromol Biosci **9,** 1194, 2009.
99. Benton, A., DeForest, A., Vivekanandan, V., and Anseth, S. Photocrosslinking of gelatin macromers to synthesize porous hydrogels that promote valvular interstitial cell function. Tissue EngPart A **15,** 3221, 2009.
100. Farrell, E., O'Brien, F., Doyle, P., and Fischer, J. A collagen-glycosaminoglycan scaffold supports adult rat mesenchymal stem cell differentiation along osteogenic and chondrogenic routes. Tissue Eng **12,** 459, 2006.
101. Yuan, T., Zhang, L., Li, K., Fan, H., Fan, Y., and Liang, J. Collagen hydrogel as an immunomodulatory scaffold in cartilage tissue engineering. J Biomed Mater Res B Appl Biomater **102,** 337, 2014.
102. Zheng, L., Sun, J., Chen, X., Wang, G., Jiang, B., and Fan, H. In vivo cartilage engineering with collagen hydrogel and allogenous chondrocytes after diffusion chamber implantation in immunocompetent host. Tissue Eng Part A **15,** 2145, 2009.
103. Villanueva, I., Gladem, S., Kessler, J., and Bryant, S. Dynamic loading stimulates chondrocyte biosynthesis when encapsulated in charged hydrogels prepared from poly (ethylene glycol) and chondroitin sulfate. Matrix Biol **29,** 51, 2010.
104. Bryant, J., Davis-Arehart, A., Luo, N., Shoemaker, R., and Anseth, S. Synthesis and characterization of photopolymerized multifunctional hydrogels: water-soluble poly(vinyl alcohol) and chondroitin sulfate macromers for chondrocyte encapsulation. Macromolecules **37,** 6726, 2004.
105. Strehin, I., Nahas, Z., Arora, K., Nguyen, T., and Elisseeff, J. A versatile pH sensitive chondroitin sulfate–PEG tissue adhesive and hydrogel. Biomaterials **10,** 2788, 2010.
106. Segura, T., Anderson, B., Chung, P., and Webber, R. Crosslinked hyaluronic acid hydrogels: a strategy to functionalize and pattern. Biomaterials **26,** 359, 2005.
107. Burdick, A., Chung, C., Jia, X., and Langer, R. Controlled degradation and mechanical behavior of photopolymerized hyaluronic acid networks. Biomacromolecules **6,** 386, 2004.

108. Suh, J., and Matthew, H. Application of chitosan-based polysaccharide biomaterials in cartilage tissue engineering: a review. Biomaterials **21,** 2589, 2000.
109. Hong, Y., Song, H., Gong, Y., Mao, Z., Gao, C., and Shen, J. Covalently crosslinked chitosan hydrogel: properties of in vitro degradation and chondrocyte encapsulation. Acta Biomater **3,** 23, 2007.
110. Tan, P., Marra, G., Tan, H., Rubin, P., and Pittsburgh, U. Injectable in situ forming biodegradable chitosan-hyaluronic acid based hydrogels for adipose tissue regeneration. Organogenesis **6,** 173, 2010.
111. Nettles, L., Elder, S., and Gilbert, J. Potential use of chitosan as a cell scaffold material for cartilage tissue engineering. Tissue Eng **8,** 1009, 2002.
112. Zhang, L., Li, K., Xiao, W., Zheng, L., Xiao, Y., and Fan, H. Preparation of collagen–chondroitin sulfate–hyaluronic acid hybrid hydrogel scaffolds and cell compatibility in vitro. Carbohyd Polym **84,** 118, 2011.
113. Lee, H., Lee, J., Chansakul, T., Yu, C., and Elisseeff, J. Collagen mimetic peptide-conjugated photopolymerizable PEG hydrogel. Biomaterials **27,** 5268, 2006.
114. Kwon, J., Yoon, S., Shim, S., Park, J., and Min, K. Injectable extracellular matrix hydrogel developed using porcine articular cartilage. Int J Pharm **454,** 183, 2013.
115. Chen, Y., Chen, R., Jhan, H., and Liu, D. Development and characterization of acellular extracellular matrix scaffolds from porcine menisci for use in cartilage tissue engineering. Tissue Eng Part C Methods Jun **10,** 2015.
116. Visser, J., Levett, P., and Moller, N. Crosslinkable hydrogels derived from cartilage, meniscus and tendon tissue. Tissue Eng Part A **21,** 1195, 2015.
117. Fan, H., Zhang, C., Li, J., Bi, L., Qin, L., and Wu, H. Gelatin microspheres containing TGF-β3 enhance the chondrogenesis of mesenchymal stem cells in modified pellet culture. Biomacromolecules **9,** 927, 2008.
118. Moioli, E., Hong, L., Guardado, J., and Clark, P. Sustained release of TGF β 3 from PLGA microspheres and its effect on early osteogenic differentiation of human mesenchymal stem cells. Tissue Eng **12,** 537, 2006.
119. Wenk, E., Meinel, A., Wildy, S., Merkle, H., and Meinel, L. Microporous silk fibroin scaffolds embedding PLGA microparticles for controlled growth factor delivery in tissue engineering. Biomaterials **30,** 2571, 2009.
120. Place, E., Nair, R., Chia, H., Szulgit, G., Lim, E., and Stevens, M. Latent TGFβ Hydrogels for Cartilage Tissue Engineering. Adv Health Mater **1,** 480, 2012.
121. Nguyen, L., Kudva, A., Saxena, N., and Roy, K. Engineering articular cartilage with spatially-varying matrix composition and mechanical properties from a single stem cell population using a multi-layered hydrogel. Biomaterials **32,** 6946, 2011.
122. Nguyen, L., Kudva, A., Guckert, N., Linse, K., and Roy, K. Unique biomaterial compositions direct bone marrow stem cells into specific chondrocytic phenotypes corresponding to the various zones of articular cartilage. Biomaterials **32,** 1327, 2011.
123. Karimi, T., Barati, D., Karaman, O., and Moeinzadeh, S. A developmentally inspired combined mechanical and biochemical signaling approach on zonal lineage commitment of mesenchymal stem cells in articular cartilage regeneration. Integr Biol (Camb) **7,** 112, 2015.
124. Bryant, S., and Anseth, K. Hydrogel properties influence ECM production by chondrocytes photoencapsulated in poly (ethylene glycol) hydrogels. J Biomed Mater Res **59,** 63, 2002.
125. Zscharnack, M., Hepp, P., and Richter, R. Repair of chronic osteochondral defects using predifferentiated mesenchymal stem cells in an ovine model. Am J Sports Med **38,** 1857, 2010.
126. Akens, M., and Rechenberg, B. Long term in-vivo studies of a photo-oxidized bovine osteochondral transplant in sheep. BMC Musculoskelet Disord **2,** 1471, 2001.
127. Oka, M., Noguchi, T., Kumar, P., Ikeuchi, K., and Yamamuro, T. Development of an artificial articular cartilage. Proc Inst Mech Eng H **214,** 59, 1990.
128. Bichara, D., and Zhao, X. Porous poly (vinyl alcohol)-hydrogel matrix-engineered biosynthetic cartilage. Tissue Eng Part A **17,** 301, 2010.
129. Maher, S., Doty, S., and Torzilli, P. Nondegradable hydrogels for the treatment of focal cartilage defects. J Biomed Mater Res A **83,** 145, 2007.
130. Kim, H., Jiao, A., Hwang, N., Kim, M., and Kang, D. Nanotopography-guided tissue engineering and regenerative medicine. Adv Drug Deliv Rev **65,** 536, 2013.
131. Park, J., Kim, P., Helen, W., Engler, A., and Levchenko, A. Control of stem cell fate and function by engineering physical microenvironments. Integr Biol (Camb) **4,** 1008, 2012.
132. McNamara, L., McMurray, R., and Biggs, M. Nanotopographical control of stem cell differentiation. J Tissue Eng **1,** 13, 2010.
133. Kim, D., Provenzano, P., and Smith, C. Matrix nanotopography as a regulator of cell function. J Cell Biol **197,** 351, 2012.
134. Dalby, M., Biggs, M., and Gadegaard, N. Nanotopographical stimulation of mechanotransduction and changes in interphase centromere positioning. J Cell Biochem **100,** 326, 2007.
135. Ingber, D. Cellular mechanotransduction: putting all the pieces together again. FASEB J **20,** 811, 2006.
136. Orr, A., Helmke, B., Blackman, B., and Schwartz, M. Mechanisms of mechanotransduction. Dev Cell **10,** 11, 2006.
137. Kim, D., Han, K., Gupta, K., Kwon, K., and Suh, K. Mechanosensitivity of fibroblast cell shape and movement to anisotropic substratum topography gradients. Biomaterials **30,** 5433, 2009.
138. Wang, N., Tytell, J, and Ingber, D. Mechanotransduction at a distance: mechanically coupling the extracellular matrix with the nucleus. Nat Rev Mol Cell Biol **10,** 75, 2009.
139. Wozniak, M., and Chen, C. Mechanotransduction in development: a growing role for contractility. Nat Rev Mol Cell Biol **10,** 34, 2009.
140. Buttafoco, L., Kolkman, N., Engbers-Buijtenhuijs, P., Poot, A., Dijkstra, P., and Vermes, I. Electrospinning of collagen and elastin for tissue engineering applications. Biomaterials **27,** 724, 2006.
141. Dong, B., Arnoult, O., Smith, M., abd Wnek, E. Electrospinning of collagen nanofiber scaffolds from benign solvents. Macromol Rapid Commun **30,** 539, 2009.
142. Barnes, P., Pemble, W., Brand, D., Simpson, D., and Bowlin, G. Cross-linking electrospun type II collagen tissue engineering scaffolds with carbodiimide in ethanol. Tissue Eng **13,** 1593, 2007.
143. Matthews, J., Wnek, G., Simpson, D., and Bowlin, G. Electrospinning of collagen nanofibers. Biomacromolecules **3,** 232, 2002.

144. Chen, Z., Mo, X., and Qing, F. Electrospinning of collagen–chitosan complex. Mater Lett **61,** 3490, 2007.
145. Sell, S., Wolfe, P., Garg, K., McCool, J., Rodriguez, I., and Bowlin, G. The use of natural polymers in tissue engineering: a focus on electrospun extracellular matrix analogues. Polymers **2,** 522, 2010.
146. Ryan, D., and Nilsson, B. Self-assembled amino acids and dipeptides as noncovalent hydrogels for tissue engineering. Polym Chem **3,** 18, 2011.
147. Rajagopal, K., and Schneider, J. Self-assembling peptides and proteins for nanotechnological applications. Curr Opin Struct Biol **14,** 480, 2004.
148. Lakshmanan, A., Zhang, S., and Hauser, C. Short self-assembling peptides as building blocks for modern nanodevices. Trends Biotechnol **30,** 155, 2012.
149. Adler-Abramovich, L., Aronov, D., and Beker, P. Self-assembled arrays of peptide nanotubes by vapour deposition. Nature **4,** 849, 2009.
150. Kim, J., Lee, S., Kim, S., and Tatman P. Effect of self-assembled peptide–mesenchymal stem cell complex on the progression of osteoarthritis in a rat model. Int J Nanomedicine **9,** 141, 2014.
151. Wise, J., Yarin, A., Megaridis, C., and Cho, M. Chondrogenic differentiation of human mesenchymal stem cells on oriented nanofibrous scaffolds: engineering the superficial zone of articular cartilage. Tissue Eng Part A **15,** 913, 2009.
152. Chen, T., Hilton, M., Brown, E., Zuscik, M., and Awad, H. Engineering superficial zone features in tissue engineered cartilage. Biotechnol Bioeng **110,** 1476, 2013.
153. Baker, B., Nerurkar, N., and Burdick J. Fabrication and modeling of dynamic multi-polymer nanofibrous scaffolds. J Biomech Eng **131,** 10, 2009.
154. Cont, L., Grant, D., Scotchford, C., Todea, M., and Popa, C. Composite PLA scaffolds reinforced with PDO fibers for tissue engineering. J Biomater Appl **27,** 707, 2013.
155. Matthews, J., Boland, E., Wnek, G., Simpson, D., and Bowlin, G. Electrospinning of collagen type II: a feasibility study. J Bioact Compat Polym **18,** 125, 2003.
156. Baker, B., Gee, A., Metter, R., Nathan, A., and Marklein, R. The potential to improve cell infiltration in composite fiber-aligned electrospun scaffolds by the selective removal of sacrificial fibers. Biomaterials **29,** 2348, 2008.
157. Jeannine, C., Gibson, M., Monagle, S., and Zachary P. Bioinspired nanofibers support chondrogenesis for articular cartilage repair. Proc Natl Acad Sci **109,** 10012, 2012.
158. Baker, B., Shah, R., and Huang, A. Dynamic tensile loading improves the functional properties of mesenchymal stem cell-laden nanofiber-based fibrocartilage. Tissue Eng Part A **17,** 1445, 2011.
159. Baker, B., Handorf, A., and Ionescu, L. New directions in nanofibrous scaffolds for soft tissue engineering and regeneration. Expert Rev Med Devices **6,** 515, 2009.
160. Baker, B., and Mauck, R. The effect of nanofiber alignment on the maturation of engineered meniscus constructs. Biomaterials **28,** 1967, 2007.
161. Li, W., Tuli, R., Okafor, C., Derfoul, A., and Danielson, K. A three-dimensional nanofibrous scaffold for cartilage tissue engineering using human mesenchymal stem cells. Biomaterials **26,** 599, 2005.
162. McCullen, S., Autefage, H., and Callanan, A. Anisotropic fibrous scaffolds for articular cartilage regeneration. Tissue Eng Part A **18,** 2073, 2012.
163. Yoo, H., Kim, T., and Park, T. Surface-functionalized electrospun nanofibers for tissue engineering and drug delivery. Adv Drug Deliv Rev **61,** 1033, 2009.
164. Stendahl, J. Growth factor delivery from self-assembling nanofibers to facilitate islet transplantation. Transplantation **86,** 478, 2008.
165. Kim, T., Chung, H., and Park, T. Macroporous and nanofibrous hyaluronic acid/collagen hybrid scaffold fabricated by concurrent electrospinning and deposition/leaching of salt particles. Acta Biomater **4,** 1611, 2008.
166. Yang, Y., Wimpenny, I., and Ahearne, M. Portable nanofiber meshes dictate cell orientation throughout three-dimensional hydrogels. Nanomedicine **7,** 131, 2011.
167. Jang, J., Lee, J., Seol, Y., Jeong, Y., and Cho, D. Improving mechanical properties of alginate hydrogel by reinforcement with ethanol treated polycaprolactone nanofibers. Composites Part B **45,** 1216, 2013.
168. Kai, D., Prabhakaran, M., Stahl, B., Eblenkamp, M., Wintermantel, E., and Ramakrishna, S. Mechanical properties and behavior of nanofiber–hydrogel composites for tissue engineering applications. Nanotechnology **23,** 9, 2012.
169. Zhou, C., and Wu, Q. A novel polyacrylamide nanocomposite hydrogel reinforced with natural chitosan nanofibers. ColloidsSurf B Biointerfaces **84,** 155, 2011.
170. Gibson, M., Pierre, B., Christopher, L., Hai-Quan, M., and Lorenzo, M. Biomimetrics of the extracellular metrix: an integrated three-dimensional fiber-hydrogel composite for cartilage tissue engineering. Smart Struct Syst **7,** 213, 2012.
171. Moroni, L., Schotel, R., Hamann, D., de Wijn, J., and van Blitterswijk, C. 3D fiber-deposited electrospun integrated scaffolds enhance cartilage tissue formation. Adv Funct Mater **18,** 53, 2008.
172. Shim, J., Kim, J., Park, M., Park, J., and Cho, D. Development of a hybrid scaffold with synthetic biomaterials and hydrogel using solid freeform fabrication technology. Biofabrication **3,** 3, 2011.
173. Tao, X., Kyle, B., Mohammad, A., Dice, D., and Yoo, J. Hybrid printing of mechanically and biologically improved constructs for cartilage tissue engineering applications. Biofabrication **5,** 1, 2012.
174. Levato, R., Visser, J., Planell, J., Engel, E., and Malda, J. Biofabrication of tissue constructs by 3D bioprinting of cell-laden microcarriers. Biofabrication **6,** 1758, 2014.
175. Shim, J., Lee, J., Kim, J., and Cho, D. Bioprinting of a mechanically enhanced three-dimensional dual cell-laden construct for osteochondral tissue engineering using a multi-head tissue/organ building system. J Micromech Microeng **22,** 8, 2012.
176. Chang, Y., Gu, H., Kobayashi, M., and Oka, M. Comparison of the bony ingrowth into an osteochondral defect and an artificial osteochondral composite device in load-bearing joints. Knee **5,** 205, 998.
177. Bailey, A., Sims, T., Ebbesen, E., and Mansell, J. Age-related changes in the biochemical properties of human cancellous bone collagen: relationship to bone strength. Calcif Tissue Int **65,** 203, 1999.
178. Nilas, L., Nørgaard, H., Pødenphant, J., Gotfredsen, A., and Christiansen, C. Bone composition in the distal forearm. Scand J Clin Lab Invest **47,** 41, 2010.
179. Fratzl, P., Gupta, H., and Paschalis, E. Structure and mechanical quality of the collagen–mineral nanocomposite in bone. J Mater Chem **14,** 14, 2004.

180. Nemeth, C., Janebodin, K., and Yuan, A. Enhanced chondrogenic differentiation of dental pulp stem cells using nanopatterned PEG-GelMA-HA hydrogels. Tissue Eng Part A **20,** 2817, 2014.
181. Mouthuy, P., El-Sherbini, Y., and Cui, Z. Layering PLGA-based electrospun membranes and cell sheets for engineering cartilage–bone transition. J Tissue Eng Regen Med **11,** 2013.
182. Qi, Y., Zhao, T., Xu, K., Dai, T., and Yan, W. The restoration of full-thickness cartilage defects with mesenchymal stem cells (MSCs) loaded and cross-linked bilayer collagen scaffolds on rabbit model. Mol Biol Rep **39,** 1231, 2012.
183. Harley, B., Lynn, A., Wissner-Gross, Z., Bonfield, W., Yannas, I., and Gibson, L. Design of a multiphase osteochondral scaffold. II. Fabrication of a mineralized collagen-glycosaminoglycan scaffold. J Biomed Mater Res A **92,** 1066, 2009.
184. Yunos, D., Ahmad, Z., Salih, V., and Boccaccini, A. Stratified scaffolds for osteochondral tissue engineering applications: electrospun PDLLA nanofibre coated bioglass(R)-derived foams. J Biomater Appl **27,** 5, 2012.
185. Galperin, A., Oldinski, R., Florczyk, S., and Bryers, J. Integrated bi-layered scaffold for osteochondral tissue engineering. Adv Healthcare Mater **2,** 872, 2013.
186. Efe, T., Theisen, C., and Fuchs, S. Cell-free collagen type I matrix for repair of cartilage defects—clinical and magnetic resonance imaging results. Knee Surg Sports Traumatol Arthrosc **20,** 1915, 2012.
187. Schneider, U., Rackwitz, L., and Andereya, S. A prospective multicenter study on the outcome of type I collagen hydrogel–based autologous chondrocyte implantation (CaReS) for the repair of articular cartilage defects in the knee. Am J Sports Med **39,** 12, 2011.
188. Stanish, W., McCormack, R., Forriol, F., and Mohtadi, N. Novel scaffold-based BST-CarGel treatment results in superior cartilage repair compared with microfracture in a randomized controlled trial. J Bone Joint Surg Am **95,** 1640, 2013.
189. Filardo, G., Kon, E, Di Martino, A., and Busacca, M. Treatment of knee osteochondritis dissecans with a cell-free biomimetic osteochondral scaffold clinical and imaging evaluation at 2-year follow-up. Am J Sports Med **41,** 1786, 2013.
190. Wang, D., Varghese, S., Sharma, B., Strehin, I., Fermanian, S. Multifunctional chondroitin sulphate for cartilage tissue–biomaterial integration. Nat Mater **6,** 385, 2007.
191. Simson, J., Crist, J., Strehin, I., Lu, Q., and Elisseeff, J. An orthopedic tissue adhesive for targeted delivery of intraoperative biologics. J Orthop Res **31,** 392, 2012.
192. Kruuml, J., Hondke, S., Endres, and Kaps, C. Human platelet-rich plasma stimulates migration and chondrogenic differentiation of human subchondral progenitor cells. J Orthop Res **30,** 845, 2012.
193. Roberts, S., Weightman, B., Urban, J., and Chappell, D. Mechanical and biochemical properties of human articular cartilage in osteoarthritic femoral heads and in autopsy specimens. J Bone Joint Surg Br **68,** 278, 1986.
194. Sweigart, M., Zhu, C., Burt, D., and Agrawal, C. Intraspecies and interspecies comparison of the compressive properties of the medial meniscus. Ann Biomed Eng **32,** 1569, 2004.
195. Jeon, O., Song, S., Lee, K., Park, M., Lee, S., and Hahn, S. Mechanical properties and degradation behaviors of hyaluronic acid hydrogels cross-linked at various cross-linking densities. Carbohydr Polym **70,** 251, 2007.
196. Chung, C., Beecham, M., Mauck, R., and Burdick, J. The influence of degradation characteristics of hyaluronic acid hydrogels on in vitro neocartilage formation by mesenchymal stem cells. Biomaterials **30,** 4287, 2009.
197. Chung, C., Erickson, I., Mauck, R. Differential behavior of auricular and articular chondrocytes in hyaluronic acid hydrogels. Tissue Eng Part A **14,** 1121, 2008.
198. Chung, C., Mesa, J., Randolph, M., Yaremchuk, M., and Burdick, J. Influence of gel properties on neocartilage formation by auricular chondrocytes photoencapsulated in hyaluronic acid networks. J Biomed Mater Res A **77,** 518, 2006.
199. Hwang, N., Varghese, S., Lee, H., and Theprungsirikul, P. Response of zonal chondrocytes to extracellular matrix-hydrogels. FEBS Lett **581,** 4172, 2007.
200. Holloway, J., Lowman, A., and Palmese, G. Mechanical evaluation of poly (vinyl alcohol)-based fibrous composites as biomaterials for meniscal tissue replacement. Acta Biomater **6,** 4716, 2010.
201. Spiller, K., Laurencin, S., Charlton, D., and Maher, S. Superporous hydrogels for cartilage repair: evaluation of the morphological and mechanical properties. Acta Biomater **4,** 17, 2008.
202. Yu, F., Cao, X., Zeng, L., Zhang, Q., and Chen, X. An interpenetrating HA/G/CS biomimic hydrogel via Diels-Alder click chemistry for cartilage tissue engineering. Carbohydr Polym **97,** 188 2013.
203. Hutson, C., Nichol, J., Aubin, H., Bae, H., Yamanlar, S., and Al-Haque, S. Synthesis and characterization of tunable poly(ethylene glycol): gelatin methacrylate composite hydrogels. Tissue Eng Part A **17,** 1713, 2011.
204. Bryant, S., Arthur, J., and Anseth, K. Incorporation of tissue-specific molecules alters chondrocyte metabolism and gene expression in photocrosslinked hydrogels. Acta Biomater **1,** 243, 2005.
205. Colburn, J., Gibson, M., Pierre, B., Christopher, L., Hai-Quan, M., Lorenzo, M., *et al.* Biomimetrics of the extracellular metrix: an integrated three-dimensional fiber-hydrogel composite for cartilage tissue engineering. Smart Struct Syst **7,** 2012.

Address correspondence to:
Deok-Ho Kim, PhD
Department of Bioengineering
University of Washington
Box 355061
Seattle, WA 98195

E-mail: deokho@uw.edu

Albert O. Gee, MD
Department of Orthopaedics and Sports Medicine
University of Washington
Box 354060
Seattle, WA 98195

E-mail: ag112@uw.edu

Received: March 24, 2015
Accepted: July 8, 2015
Online Publication Date: October 14, 2015